ISEF 2005 - XII International Symposium on Electromagnetic Fields
in Mechatronics, Electrical and Electronic Engineering
Baiona, Spain, September 15-17, 2005

STRUCTURE-DYNAMIC SIMULATION OF AN INDUCTION FURNACE WITH RESPECT TO FLUID-SOLID INTERACTION OF LIQUID METAL AND CRUCIBLE

M. C. Schöning, D. van Riesen, H. Brunnberg, K. Hameyer

Institute of Electrical Machines, RWTH Aachen University
Schinkelstraße 4, D-52062 Aachen, Germany
Marc.Schoening@iem.rwth-aachen.de

***Abstract* – Induction furnaces are used for melting purposes of electrically conducting material such as steel or aluminium. Due to the high power consumption of such devices evoking strong vibrations, the electromagnetically excited acoustic noise states an important criteria for their design. This paper presents an approach for the structure-dynamic simulation of an induction furnace representing the basis for the acoustic computation. The presented approach is performing an electromagnetic simulation taking eddy currents in the coils and in the melt into account. The resulting Lorentz forces are transformed to a structure-dynamic model capturing the approximation of the interaction between the liquid metal and the crucible. The simulation procedure is terminated computing the body sound and airborne sound.**

Introduction

The simulation is performed by means of the Finite-Element Method (FEM). In the first step, the Lorentz forces are computed. The resulting forces are transformed to a structure-dynamic model consisting of first order hexahedral elements. With this model the harmonic response analysis is performed determining the dynamic behaviour of the induction furnace caused by the Lorentz forces. Based on the deformation an acoustic simulation is performed to calculate the body sound and airborne sound.

Electromagnetic Simulation

Due to the sinusoidal currents in the coils, a time-harmonic approach is used. The coil windings are water-cooled solid conductors. Therefore, the coils are considered as eddy current regions. The melt is assumed to be an eddy current region as well. For the computation, an edge-element formulation with two vector potentials (A,T) is applied [2][3]. In order to reduce the computation time, a symmetric cut out of 30° is sufficient to model the furnace. The Lorentz force density is defined by:

$$\vec{f}(t) = \left(\vec{J}(t) \times \vec{B}(t)\right) \quad . \tag{1}$$

The force density becomes maximal, when the fields are perpendicular to each other. Assuming a rotationally symmetric geometry, the current density $\vec{J}(t)$ has a pure circular component and the flux density $\vec{B}(t)$ has an axial and a radial component:

$$\vec{f}_{=}(t) = \vec{J} \times \vec{B} = \begin{pmatrix} 0 \\ J_\varphi \\ 0 \end{pmatrix} \times \begin{pmatrix} B_r \\ 0 \\ B_z \end{pmatrix} = \begin{pmatrix} J_\varphi \cdot B_z \\ 0 \\ -J_\varphi \cdot B_r \end{pmatrix} \quad . \tag{2}$$

As equation (2) shows, the force has no circular component. Applying the product rule to (1) yields by using (2):

$$f(t) = \frac{1}{2} \cdot \hat{J}_{\varphi} \cdot \left[\underbrace{\begin{pmatrix} \hat{B}_Z \cdot \sin(2\omega t + \varphi_J + \varphi_{B_Z}) \\ 0 \\ \hat{B}_r \cdot \sin(2\omega t + \varphi_J + \varphi_{B_r}) \end{pmatrix}}_{\textit{Alternating Component}} + \underbrace{\begin{pmatrix} \hat{B}_Z \cdot \sin(\varphi_J - \varphi_{B_Z}) \\ 0 \\ \hat{B}_r \cdot \sin(\varphi_J - \varphi_{B_r}) \end{pmatrix}}_{\textit{Static Component}} \right] . \qquad (3)$$

The static component is important for the flow computation in the melt and the coupled calculation of the surface curvature of the bath. The alternating component leads to an oscillation amplitude resulting in sonic radiation. Therefore, both components are required for the simulation. Fig. 1a) shows the resulting flux-density distribution and Fig. 1b) shows the Lorentz-force density distribution.

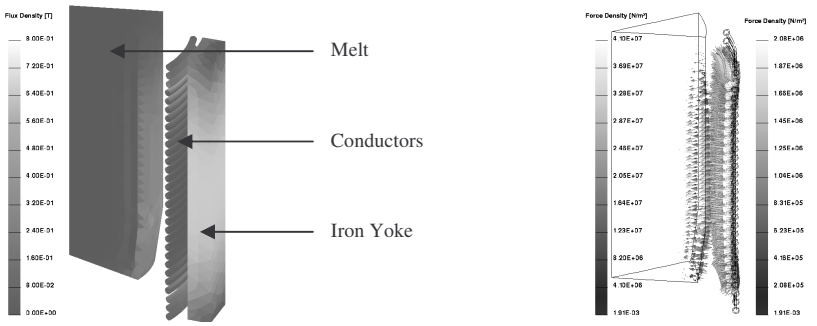

a) Flux density distribution. b) Force density distribution.

Fig. 1: Results of the electromagnetic simulation.

Structure-Dynamic Simulation

The smallest symmetry of the relevant structure-dynamic components of the furnace is 180°. The applied forces determined by the electromagnetic computation are transformed to this mechanical model. There are two approaches to simulate the structure-dynamic behaviour of a geometry. The first is a modal analysis followed by a modal superposition computation and the second is a harmonic analysis (Fig. 7). The advantage of the modal analysis and modal superposition is the short computation time, disadvantage is the necessity for symmetric system matrices. In case of the induction furnace regarding fluid-solid interaction, which results in a dense stiffness matrix [1], a full harmonic response analysis is required. The Helmholtz equation describes the distribution of oscillations in a material:

$$\Delta \underline{p} + k^2 \underline{p} = 0, \qquad (4)$$

where $k = \frac{\omega}{c}$ represents the wave number. Equation (4) is multiplied by a change of pressure δp and integrated over the volume V. Applying Gauss theorem leads to the following equation:

$$\frac{1}{c^2} \cdot \int_V \delta p \cdot \frac{\partial^2 p}{\partial t^2} dV + \int_V \nabla \cdot (\delta p \cdot \nabla p) dV = \int_S \delta p \cdot \nabla p \, d\vec{S} = \int_S \delta p \cdot \nabla p \cdot \vec{n}_S \, dS. \qquad (5)$$

S is the surface of the boundary layer and $\vec{n}_S$ the corresponding normal vector. The relation between the pressure $\underline{p}$ (melt) and the deformation $\underline{u}$ (structure) is given by:

$$\Delta \underline{p} \cdot \vec{n}_S = -p_0 \cdot \omega^2 \underline{\vec{u}} \cdot \vec{n}_S. \qquad (6)$$

This yields the discretrised lossy wave equation:

$$\underline{M}^{p} \cdot \ddot{\underline{p}} + \underline{C}^{p} \cdot \dot{\underline{p}} + \underline{K}^{p} \cdot \underline{p} + p_0 \cdot \underline{R}^{T} \cdot \ddot{\underline{u}} = 0. \tag{7}$$

$\underline{K}^{p}$ is the stiffness matrix, $\underline{C}^{p}$ is the damping matrix and $\underline{M}^{p}$ is the mass matrix of the fluid material. $\underline{R}$ is the coupling matrix for the fluid-solid interaction. The pressure node vector is represented by $\underline{p}$ and the deformation node vector is represented by $\underline{u}$. Finally a common formulation regarding the deformation of the structure and the behaviour of the fluid material is required:

$$\underline{K}^{u} \cdot \underline{u} + \underline{C}^{u} \cdot \dot{\underline{u}} + \underline{M}^{u} \cdot \ddot{\underline{u}} - \underline{R} \cdot \underline{p} = \underline{G}. \tag{8}$$

In equation (8), $\underline{G}$ represents the global load vector. The other matrix notations are similar to equation (7) but they are related to the solid material. Equation (7) and (8) are combined describing the field problem for the calculation of the fluid-solid interaction:

$$\begin{bmatrix} \underline{M}^{u} & 0 \\ \underline{M}^{fs} & \underline{M}^{p} \end{bmatrix} \cdot \begin{pmatrix} \ddot{\underline{u}} \\ \ddot{\underline{p}} \end{pmatrix} + \begin{bmatrix} \underline{C}^{u} & 0 \\ 0 & \underline{C}^{p} \end{bmatrix} \cdot \begin{pmatrix} \dot{\underline{u}} \\ \dot{\underline{p}} \end{pmatrix} + \begin{bmatrix} \underline{K}^{u} & \underline{K}^{fs} \\ 0 & \underline{K}^{p} \end{bmatrix} \cdot \begin{pmatrix} \underline{u} \\ \underline{p} \end{pmatrix} = \begin{pmatrix} \underline{G} \\ \underline{0} \end{pmatrix}. \tag{9}$$

$\underline{M}^{fs}$ is defined as $p_0 \underline{R}^{T}$ and $\underline{K}^{fs}$ as $-\underline{R}$. Equation (6) is to be solved for each single frequency in range from 0 Hz to 2000 Hz. Two examples of the resulting deformation are shown in Fig. 2.

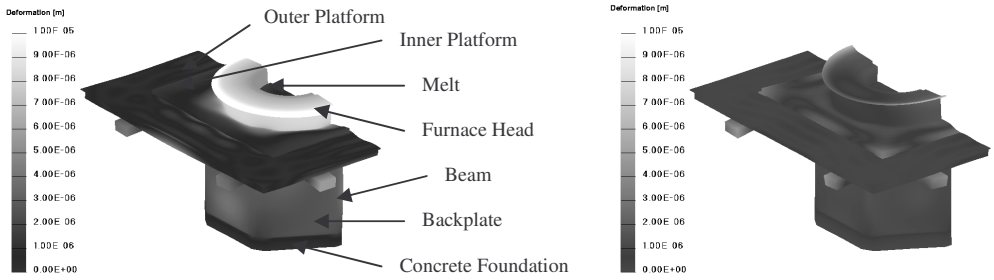

a) Real component of deformation at 306 Hz.

b) Real component of deformation at 470 Hz.

Fig. 2: Results of the structure-dynamic simulation.

The deformation at the boundary layer of the melt is shown in Fig. 3.

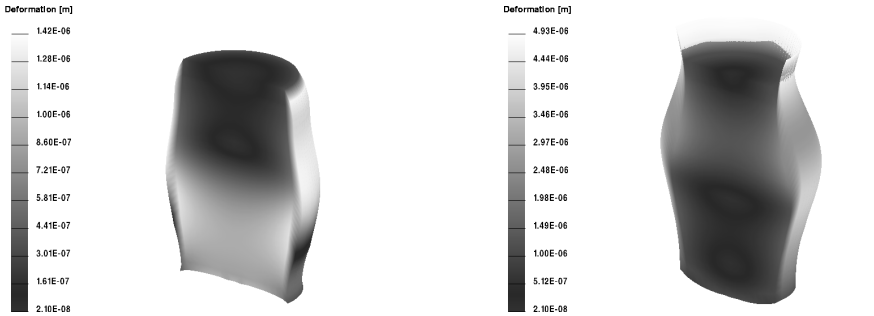

a) Real component of deformation of the melt.

b) Imaginary component of deformation of the melt.

Fig. 3: Results of structural-dynamic simulation in the melt.

Acoustic Simulation

The body sound is calculated by means of the following equation [4]:

$$L_{Sh^2} = 10\log\left(\frac{\Omega^2 \sum_{p=1}^{N_{el}} \int_{S_p} \left|v^{(p)}(\Omega)\cdot n^{(p)}\right|^2 dS}{S_0 {h_0}^2}\right). \qquad (10)$$

The body sound calculation with its short computation time is a well suited method to identify problematic frequencies. Fig. 4 shows the results for the induction furnace in range from 0 Hz to 2000 Hz.

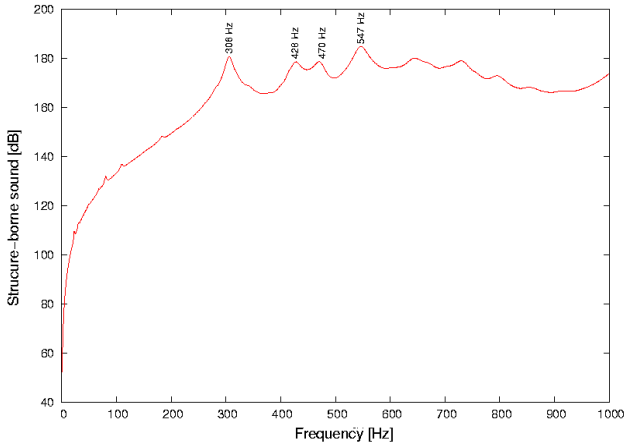

Fig. 4: Results of the structure-borne sound computation.

For the identified peaks, an airborne sound simulation is performed employing a Boundary-Element model consisting only of the surface of the induction furnace.

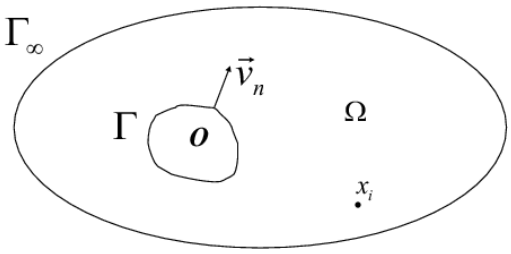

Fig. 5: Derivation of the integral equation.

Fig. 5 shows the basic approach to derive the integral equation needed for the airborne sound simulation. Γ represents a flat surface with a distinct normal vector of the irradiating object o. Ω marks the surrounding area, with Γ_∞ the border in infinity. Starting with the Helmholtz equation (4), which describe the sound pressure in the area Ω, a weighting function is introduced resulting in

$$u^* = \frac{e^{-jkr}}{4\cdot\pi\cdot r} \qquad (11)$$

for an isotropic medium in the three-dimensional case. The computation leads to the final equation:

$$c_i \cdot \underline{p}(x_i) + \int_\Gamma \underline{p} \cdot \frac{\partial u^*}{\partial n}\, d\Gamma = -j\omega\rho \cdot \int_\Gamma u^* \underline{v}\, d\Gamma \quad . \tag{12}$$

The coefficient c_i is defined as:

$$c_i = \begin{cases} 0, & x_i \in O \\ \dfrac{\theta_i}{4\pi}, & x_i \in \Gamma \\ 1, & x_i \in \Omega \end{cases} \tag{13}$$

and the sound particle velocity is defined as

$$\underline{v} = \frac{1}{j\omega\rho} \cdot \frac{\partial \underline{p}}{\partial n} \cdot \vec{e}_n \quad . \tag{14}$$

In Fig. 6, the irradiated sound level at 306 Hz and 428 Hz are shown. From the sound level distribution, the components of the induction furnace can be classified acoustically. Therefore, the acoustic behaviour of each single component can be optimized. Besides the sound level distribution the sound power is calculated. Therefore, the sound intensity is computated on a spherical seat surrounding the induction furnace. Afterwards an integration over the spherical seat is required. To obtain a decibel value, the following equation is used:

$$L_W = 10\log\left(\frac{P}{P_0}\right) \quad . \tag{15}$$

P_0 is defined as $10^{-12} W$. The sound power is utilised to compare the different frequencies generally. At 306 Hz, the sound power is 76,095 dB. At 428 Hz, the sound power is 68,287 dB. Compared with the body sound calculation, the value at 306 Hz is also higher then the value at 428 Hz.

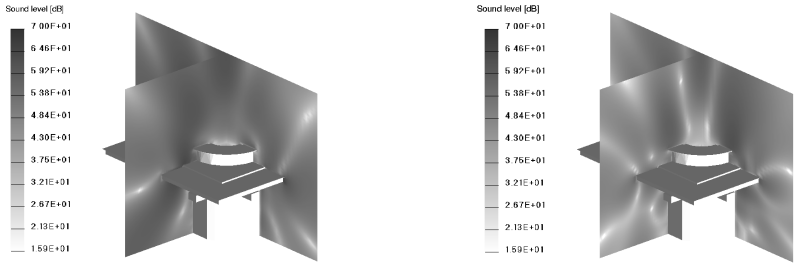

a) Airborne sound at 306 Hz. b) Airborne sound at 428 Hz.

Fig. 6: Results of the acoustic simulation.

Conclusions

The computation chain, presented in this paper represents a well suited approach to determine the structure-dynamic behaviour and the irradiated sound of induction furnaces considering the interaction of liquid metal and the crucible. To reduce computation time all possible symmetries are utilised. Thereby, the body-sound computation provides the possibility to evaluate the acoustic behaviour of the furnace with only marginal calculation time. Due to large computational effort, the acoustic simulation is

performed only for the identified peaks of the body-sound calculation. In Fig. 7, the dependencies of the computation steps are shown.

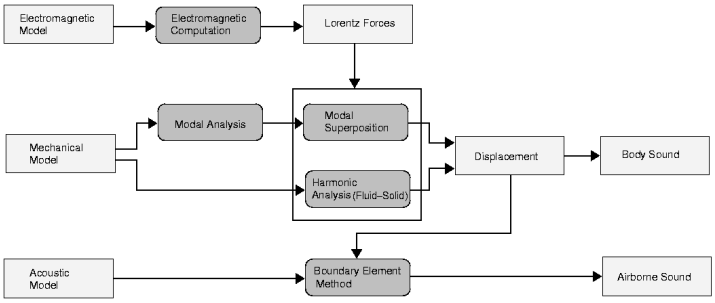

Fig. 7: Computation chain.

Different modifications are made to the induction furnace, and simulations of these variants are performed to reduce the irradiated sound of the furnace. At first, a rubber buffer between inner and outer platform is implemented. In addition the material density of the concrete as well as the thickness of the back plate, of the platform and of the beams are varied. The results (Fig. 8) show that a rubber buffer decreases the sound power significantly. Doubling the back plate thickness reduces the irradiated sound up to 480 Hz. Since the current frequency can reach 250 Hz depending on the melt level, the frequency of the resulting force is 500 Hz. Therefore, this variant is not appropriate for a completely filled induction furnace. At last, decreasing the concrete density reduces the sound power over the complete examined frequency spectrum marginally. All other simulated variants do not enhance the acoustic behaviour of the induction furnace.

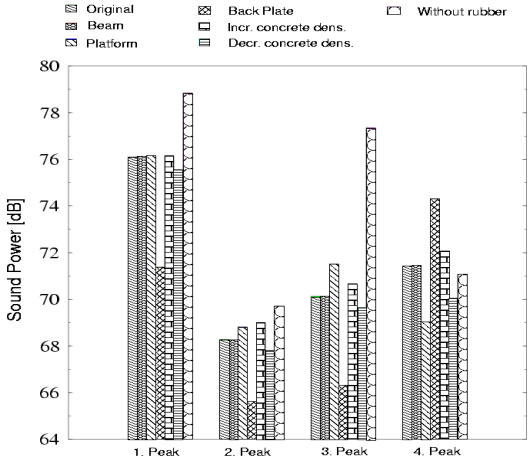

Fig. 8: Results of different modifications.

References

[1] W. Kanok-Nukulchai, B. T. Tam. *Structure Fluid Interaction Model of Tuned Liquid Dampers*, International Journal for Numerical Methods in Engineering, Vol. 46, pp 1541-1558, 1999.

[2] O. Bíró, *Edge element formulations of eddy current problems*, Computational Methods in Applied Mechanics Eng., vol. 169, pp. 391-405, 1999.

[3] D. van Riesen, G. Henneberger, *Combining electrical and mechanical analysis in an object-oriented package for the coupled calculation of an induction furnace*, Proceedings of the 10th International Symposium on Numerical Field Calculation in Electrical Engineering, IGTE, Graz, pp 76-77, September 2002.

[4] F. G. Kollmann, *Maschinenakustik*, Berlin, Springer Verlag, 2000.